PERGAMON International Journal of Engineering Science 37 (1999) 665–685

International Journal of Engineering Science

Analysis of microstructural fields in heterogeneous piezoelectric solids

J.Y. Li, M.L. Dunn *

Center for Acoustics, Mechanics, and Materials, Department of Mechanical Engineering, University of Colorado, Boulder, Colorado, U.S.A

Received 30 April 1998; accepted 30 May 1998
(Communicated by T. MURA)

Abstract

A theory is developed to analyze the internal fields in heterogeneous piezoelectric solids. It is used to derive expressions for mean values and variations of the internal fields due to external loading and eigenfields. The general theory is applicable to both polycrystalline ceramics as well as matrix-based composites. After the general development, the theory is applied to multiphase matrix-based piezoelectric composites, and explicit relations are obtained for two-phase composites. Exact connections are established between the effective thermal properties and the effective electroelastic moduli, and these agree with previous results of Benveniste [3] and Dunn [15] obtained by two different approaches. The stored enthalpy of the heterogeneous solid is also expressed as an explicit function of the effective thermoelectroelastic properties. Finally, to demonstrate the applicability of the theory, numerical results for average fields and field variations are presented for a two-phase composite consisting of continuous piezoelectric fibers embedded in a polymer matrix.

1. Introduction

Applications of piezoelectric solids have increased dramatically in recent years, fueled largely by their many uses in active materials and structures systems. Their attractiveness stems from their inherent ability to convert electrical energy to mechanical energy and vice-versa. They are a natural choice for ultraprecise displacement transducers and actuators and their role in functional material systems is rapidly increasing.

* Corresponding author. Tel.: 001 303 492 6542; Fax: 001 303 492 3498; E-mail: dunnm@spot.colorado.edu

0020-7225/99/$ - see front matter
PII: S0020-7225(98)00091-3

An inherent property of most piezoelectric materials is that of heterogeneity; heterogeneity that exists at multiple length scales. Piezoelectric crystals often contain complicated domain configurations which are regions of different electrical polarization. The permissible configurations are dictated by the symmetry of the crystal. This results in a variation of the elastic, piezoelectric, and dielectric constants throughout the crystal; their values at a certain location depend on the orientation of the domain at that location. When a piezoelectric polycrystal is fabricated by standard ceramic processing techniques, the situation is even more complicated. Now, not only does each grain itself have a domain structure, but the arrangement of the grains in the polycrystal also leads to heterogeneity. Furthermore, upon processing the elastic, electric, and thermal anisotropy of the grains can lead to complicated internal electroelastic fields. These can include appreciable internal microstructural stresses. In order to relieve these stresses, domain reorientation and microcracking can occur and these in turn can substantially influence the overall response of the polycrystal. Furthermore, porosity often exists due to sintering and this also affects the overall behavior of the ceramic. The influence can be either good or bad [23]. At an even larger length scale, polycrystalline ceramic fibers are often embedded in a polymer matrix to form a piezoelectric composite. At this scale, it is really the effective properties of the ceramic fibers that influence the overall response of the composite. The distribution of the internal electroelastic fields in the composite microstructure of course determines the overall response. In this case, both internal electrical and mechanical fields couple. They result from external thermal, electrical, and mechanical loads.

Theoretical studies of heterogeneous piezoelectric solids have been primarily aimed at the determination of effective properties [3–8, 12–23, 25, 34, 38–40]. Regarding the analysis of internal fields, Benveniste [3, 4, 6] and Benveniste and Dvorak [8] established the existence of uniform fields in a class of piezoelectric composites and used it to derive internal consistency relations between effective moduli. Dunn [18] analyzed thermally-induced fields in electroelastic composites to obtain average fields and the effective behavior. A simple model where grains were modeled as spherical particles was proposed by Kroupa et al. [31] to describe the anisotropic distribution of internal stresses in poled PZT ceramics. Arlt [1] studied stress relief in ferroelectric ceramics based on a regular domain structure. In general, all previous works are based on the assumption of a specific microstructural geometry, and they are limited to the estimation of average fields in the phases. No attempts have been made to estimate the field fluctuations.

Significant efforts have been undertaken to study internal fields in heterogeneous elastic solids, particularly when the materials are isotropic. These include the information entropy method [30], effective medium approaches [9, 10], the use of special correlation functions [29, 35], and the multiparticle effective field method [11]. Kreher [27, 28] also established exact relations between internal elastic fields and the effective properties of heterogeneous solids. Each of these approaches deals with statistical information including average fields as well as variations of the elastic fields.

In all of the cases of heterogeneous piezoelectric media described above, the microstructure is probably most reasonably modeled as a random field, and in general it is three-dimensional. As a result, a deterministic treatment of the random internal electroelastic fields is of limited utility. In light of this, in this paper we lay the framework for a theory to model internal fields in heterogeneous piezoelectric media. We are motivated largely by the successes of Kreher and

colleagues with regard to modeling elastic microstructural stresses. With the appropriate interpretation, the results obtained here can be applied to any of the length scales discussed above, and so it is quite general in that sense. In this work we do not apply the formalism to all of these problems. Instead, to demonstrate, we apply it to the case of a two-phase composite consisting of piezoelectric fibers in a polymer matrix.

2. Basic equations and notation

We consider the piezoelectric, and thus inherently anisotropic, analog of the uncoupled theory of thermoelasticity. The electric and elastic fields are fully coupled, but temperature enters the problem only as a parameter through the constitutive equations. The field variables and material moduli are represented either by conventional indicial notation or by bold characters. The constitutive equations for stationary linear response of a thermoelectroelastic solid can be expressed as:

$$\begin{aligned}
\varepsilon_{ij} &= S_{ijkl}\sigma_{kl} + g_{kij}D_k + \varepsilon^{\mathrm{T}}_{ij},\\
(-E_i) &= g_{ijk}\sigma_{jk} - \beta_{ij}D_j + (-E^{\mathrm{T}}_i),\\
\sigma_{ij} &= C_{ijmn}(\varepsilon_{mn} - \varepsilon^{\mathrm{T}}_{mn}) + e_{nij}[(-E_n) - (-E^{\mathrm{T}}_n)],\\
D_i &= e_{imn}(\varepsilon_{mn} - \varepsilon^{\mathrm{T}}_{mn}) - \kappa_{in}[(-E_n) - (-E^{\mathrm{T}}_n)].
\end{aligned} \tag{1}$$

In Eq. (1), σ_{mn} and ε_{mn} are the elastic stress and strain, respectively; D_m and E_m are the electric displacement and field, respectively. C_{ijmn}, e_{nij}, and κ_{in} are the elastic stiffness tensor (measured in a constant electric field), the piezoelectric tensor, and the dielectric tensor (measured at a constant strain), respectively. S_{ijmn}, g_{nij}, and β_{in} are the elastic compliance, piezoelectric, and dielectric tensors obtained from inverting the C_{ijmn}, e_{nij}, and κ_{in} equations. In the constitutive equations, $(-E_i)$ is used instead of E_i as it allows the construction of a symmetric linear response matrix which will prove to be advantageous. In Eq. (1) the eigenstrains $\varepsilon^{\mathrm{T}}_{ij}$ may be due to thermal expansion or other inelastic phenomena that results in shape or volume changes. The eigenfields E^{T}_i may be caused by the pyroelectric effect, or may result from spontaneous polarization developed during crystallographic phase transformations. We can represent the eigenstrain and eigenfield as:

$$\begin{aligned}
\varepsilon^{\mathrm{T}}_{ij} &= \int_{T_0}^{T} \Delta_{ij}(T')\,\mathrm{d}T' + \varepsilon^{\mathrm{tr}}_{ij},\\
(-E^{\mathrm{T}}_i) &= \int_{T_0}^{T} \gamma_i(T')\,\mathrm{d}T' + (-E^{\mathrm{tr}}_i).
\end{aligned} \tag{2}$$

Here Δ_{ij} are the thermal expansion coefficients, γ_i are the pyroelectric coefficients, T_0 and T are the reference and actual temperatures, respectively, and ε^{tr}_{ij} and E^{tr}_{ij} are eigenstrains and eigenfields that are caused by other mechanisms, such as phase transformations. In this work, we assume that the temperature distribution is uniform over the solid while Δ_{ij}, γ_i, $\varepsilon^{\mathrm{tr}}_{ij}$, and E^{tr}_i

may, in general, vary as a result of the heterogeneous microstructure. We can and will regard $\varepsilon_{ij}^{\mathrm{T}}$ and E_i^{T} as material properties, irrespective of their particular origins.

The strain and electric field are derivable from the elastic displacement and electric potential as:

$$\begin{aligned} \varepsilon_{ij} &= \frac{1}{2}(u_{i,j} + u_{j,i}), \\ (-E_i) &= \phi_i. \end{aligned} \tag{3}$$

In addition, the equations of elastic equilibrium and Gauss' law of electrostatics (in the absence of body forces and free charge) are:

$$\begin{aligned} \sigma_{ij,j} &= 0, \\ D_{i,i} &= 0. \end{aligned} \tag{4}$$

In the solution of piezoelectric boundary value problems, it is convenient to treat the elastic and electric variables on equal footing. To this end, the notation introduced by Barnett and Lothe [27] is employed. It is similar to conventional indicial notation with the exception that both lowercase and uppercase subscripts are used as indices. Lowercase subscripts take on the range 1, 2, 3, while uppercase subscripts take on the range 1, 2, 3, 4 and repeated uppercase subscripts are summed over $1 \to 4$. With this notation, we have the following representation for the field quantities:

$$U_M = \begin{cases} u_m \\ \phi \end{cases}, \quad Z_{Mn} = \begin{cases} \varepsilon_{mn} \\ \phi,_n = -E_n \end{cases}, \quad \Sigma_{nM} \begin{cases} \sigma_{nm} & M = 1, 2, 3 \\ D_n, & M = 4. \end{cases} \tag{5}$$

The electroelastic moduli are expressed as:

$$E_{iJMn} = \begin{cases} C_{ijmn} & J, M = 1, 2, 3, \\ e_{nij} & J = 1, 2, 3;\ M = 4, \\ e_{imn} & J = 4;\ M = 1, 2, 3, \\ -\kappa_{in} & J, M = 4. \end{cases} \tag{6}$$

The inverse of E_{iJMn} is defined as F_{AbiJ}. With this shorthand notation, we can rewrite Eqs. (1), (3) and (4) as:

$$\Sigma_{iJ} = E_{iJMn}(Z_{Mn} - Z_{Mn}^{\mathrm{T}}) \quad \text{or} \quad Z_{Ab} = F_{AbiJ}\Sigma_{iJ} + Z_{Ab}^{\mathrm{T}}, \tag{7}$$

$$Z_{Mn} = U_{M,n}, \tag{8}$$

$$\Sigma_{iJ,i} = 0. \tag{9}$$

For the heterogeneous materials considered here, we define the effective thermoelectroelastic constitutive equation in a statistical sense under the assumption of macroscopic homogeneity:

$$\langle \Sigma_{iJ} \rangle = E_{iJMn}^{*}(\langle Z_{Mn} \rangle - Z_{Mn}^{*}) \tag{10}$$

or

$$\langle Z_{Ab}\rangle = F^*_{AbiJ}\langle \Sigma_{iJ}\rangle + Z^*_{Ab} \tag{11}$$

where $\langle\bullet\rangle = 1/V\int_V(\bullet)\,\mathrm{d}V$ denotes a volume average. In Eqs. (10) and (11) E^*_{iJMn} and F^*_{AbiJ} are the effective electroelastic moduli and Z^*_{Mn} are the effective eigenfields. Again, recall that Z^*_{Mn} are considered a material property.

3. General results

In this section we lay the framework for the analysis of heterogeneous piezoelectric solids by developing general results independent of a specific microstructural geometry. These results can then be applied to specific microstructural geometries. Examples include polycrystals and matrix-based composites, the latter being the subject of the following section.

3.1. Generalized Hill conditions

Consider applied traction and electric displacement boundary conditions on the surface of the heterogeneous solid, S, consistent with a uniform stress and electric displacement Σ^0_{iJ}:

$$\Sigma_{iJ}(x) = \Sigma^0_{iJ}, \quad \mathbf{x}\in S. \tag{12}$$

Making use of the averaging theorems for heterogeneous piezoelectric solids [21], we have:

$$\langle \Sigma_{iJ}\rangle = \Sigma^0_{iJ}. \tag{13}$$

A similar result exists for applied displacement–potential boundary conditions. We assume statistical homogeneity so that $\langle\bullet\rangle$ does not depend on the position, and compute the scalar quantity:

$$\begin{aligned}
\langle \Sigma_{iJ}Z_{Ji}\rangle &= \frac{1}{V}\int_V \Sigma_{iJ}(x)Z_{Ji}(x)\,\mathrm{d}\mathbf{x}\\
&= \frac{1}{V}\int_V \Sigma_{iJ}(x)U_{J,t}(\mathbf{x})\,\mathrm{d}\mathbf{x}\\
&= \frac{1}{V}\int_S \Sigma_{iJ}(x)n_i(x)U_J(x)\,\mathrm{d}\mathbf{x}\\
&= \frac{1}{V}\int_S \langle\Sigma_{iJ}\rangle n_i(x)U_J(x)\,\mathrm{d}\mathbf{x}\\
&= \langle\Sigma_{iJ}\rangle\frac{1}{V}\int_S n_i(x)U_J(x)\,\mathrm{d}\mathbf{x}\\
&= \langle\Sigma_{iJ}\rangle\frac{1}{V}\int_V Z_{Ji}(x)\,\mathrm{d}\mathbf{x}\\
&= \langle\Sigma_{iJ}\rangle\langle Z_{Ji}\rangle.
\end{aligned} \tag{14}$$

Eq. (14) is a generalization of the Hill condition for heterogeneous elastic solids [26, 27]. The only assumptions made in the derivation are that the solid is statistically homogeneous and that Eqs. (8) and (9) are applicable. As long as the fields satisfy the equilibrium equations and gradient equations, the Hill condition is satisfied. It is not required that Σ_{iJ} and Z_{Ji} are connected by specific constitutive equations. Note that the generalized Hill condition can also be proved in the case of applied displacement and electric potential boundary conditions. The generalized Hill condition of Eq. (14) serves as the foundation of much of the analysis that follows.

3.2. Residual fields and fields due to external loads

It is advantageous to split the elastic and electric fields in heterogeneous piezoelectric solids into two parts, one due to external loading and the other consisting of residual fields:

$$\Sigma_{iJ} = \Sigma^{\mathrm{I}}_{iJ} + \Sigma^{\mathrm{II}}_{iJ}, \quad Z_{Ji} = Z^{\mathrm{I}}_{Ji} + Z^{\mathrm{II}}_{Ji}. \tag{15}$$

The fields denoted by I are created solely by the external loadings, i.e. applied tractions and electric displacements that are compatible with a homogeneous field Σ^0_{iJ}. The fields denoted by II are created by the eigenfield Z^{T}_{Mn} in the absence of external loading. In view of these definitions, the averaging theorems imply:

$$\langle \Sigma^{\mathrm{I}}_{iJ} \rangle = \Sigma^0_{iJ}, \quad \langle \Sigma^{\mathrm{II}}_{iJ} \rangle = 0. \tag{16}$$

Consequently, Eq. (7) can be decomposed into two equations:

$$\Sigma^{\mathrm{I}}_{iJ} = E_{iJMn} Z^{\mathrm{I}}_{Mn}, \tag{17a}$$

$$Z^{\mathrm{I}}_{Ab} = F_{AbiJ} \Sigma^{\mathrm{I}}_{iJ}, \tag{17b}$$

$$\Sigma^{\mathrm{II}}_{iJ} = E_{iJMn}(Z^{\mathrm{II}}_{Mn} - Z^{\mathrm{T}}_{Mn}), \tag{18a}$$

$$Z^{\mathrm{II}}_{Ab} = F_{AbiJ} \Sigma^{\mathrm{II}}_{iJ} + Z^{\mathrm{T}}_{Ab}. \tag{18b}$$

Generalizing Kreher's [27] terminology, we call field I the loading field and field II the residual field. Because both fields satisfy the equilibrium and gradient equations, the generalized Hill condition applies to both the loading and residual fields.

Taking into account the boundary conditions and the effective constitutive equations, we can show:

$$\langle \Sigma^{\mathrm{I}}_{iJ} \rangle = \Sigma^0_{iJ} \tag{19a}$$

$$\langle Z^{\mathrm{I}}_{Ab} \rangle = F^*_{AbiJ} \Sigma^0_{iJ}, \tag{19b}$$

$$\langle \Sigma^{\mathrm{II}}_{iJ} \rangle = 0 \tag{20a}$$

$$\langle Z^{\mathrm{II}}_{Ab} \rangle = Z^*_{Ab}. \tag{20b}$$

Substituting Eqs. (19) and (20) into the Hill condition (14), we obtain four scalar equations:

$$\langle \Sigma^{\mathrm{I}}_{iJ} Z^{\mathrm{I}}_{Ji} \rangle = \Sigma^{0}_{iJ} F^{*}_{JicD} \Sigma^{0}_{cD}, \tag{21}$$

$$\langle \Sigma^{\mathrm{II}}_{iJ} Z^{\mathrm{I}}_{Ji} \rangle = 0, \tag{22}$$

$$\langle \Sigma^{\mathrm{I}}_{iJ} Z^{\mathrm{II}}_{Ji} \rangle = \Sigma^{0}_{iJ} Z^{*}_{Ji}, \tag{23}$$

$$\langle \Sigma^{\mathrm{II}}_{iJ} Z^{\mathrm{II}}_{Ji} \rangle = 0. \tag{24}$$

From Eqs. (22) and (23), we obtain:

$$\begin{aligned} \Sigma^{0}_{iJ} Z^{*}_{Ji} &= \langle \Sigma^{\mathrm{I}}_{iJ} Z^{\mathrm{II}}_{Ji} \rangle \\ &= \langle (Z^{\mathrm{II}}_{Ji} - Z^{\mathrm{T}}_{Ji}) E_{iJMn} Z^{\mathrm{I}}_{Mn} \rangle + \langle Z^{\mathrm{T}}_{Ji} E_{iJMn} Z^{\mathrm{I}}_{Mn} \rangle \\ &= \langle Z^{\mathrm{T}}_{Ji} \Sigma^{\mathrm{I}}_{iJ} \rangle. \end{aligned} \tag{25}$$

Eqs. (21)–(25) establish the connection between the effective moduli and a statistical description of the microstructure for heterogeneous piezoelectric solids. They play a crucial role in the subsequent analysis.

3.3. Stored enthalpy density

The stored enthalpy density in the heterogeneous solid also plays an important role in this work. We denote the average value of the stored enthalpy per unit volume by H. It can be expressed as:

$$\begin{aligned} H &= \frac{1}{2} \langle \Sigma_{iJ} (Z_{Ji} - Z^{\mathrm{T}}_{Ji}) \rangle \\ &= \frac{1}{2} \langle \Sigma^{\mathrm{I}}_{iJ} Z^{\mathrm{I}}_{Ji} \rangle + \langle \Sigma^{\mathrm{II}}_{iJ} Z^{\mathrm{I}}_{Ji} \rangle + \frac{1}{2} \langle \Sigma^{\mathrm{II}}_{iJ} (Z^{\mathrm{II}}_{Ji} - Z^{\mathrm{T}}_{Ji}) \rangle \\ &= H^{\mathrm{I}} + H^{\mathrm{II}} \end{aligned} \tag{26}$$

where

$$H^{\mathrm{I}} = \frac{1}{2} \langle \Sigma^{\mathrm{I}}_{iJ} Z^{\mathrm{I}}_{Ji} \rangle = \frac{1}{2} \Sigma^{0}_{iJ} F^{*}_{JicL} \Sigma^{0}_{cD}, \tag{27}$$

$$H^{\mathrm{II}} = \frac{1}{2} \langle \Sigma^{\mathrm{II}}_{iJ} (Z^{\mathrm{II}}_{Ji} - Z^{\mathrm{T}}_{Ji}) \rangle = -\frac{1}{2} \langle \Sigma^{\mathrm{II}}_{iJ} Z^{\mathrm{T}}_{Ji} \rangle = \frac{1}{2} \langle \Sigma^{\mathrm{II}}_{iJ} F_{JimN} \Sigma^{\mathrm{II}}_{mN} \rangle. \tag{28}$$

The last right-hand side of Eq. (28) results when we apply the constitutive Eq. (18b). Note that the stored enthalpy H^{II} depends only on the moduli $F_{JimN}(\mathbf{x})$ and $Z^{T}_{Mn}(\mathbf{x})$. Therefore, we can regard H^{II} as an effective material constant.

3.4. First order moments of the electroelastic fields

Here our aim is to obtain relations between the effective moduli of a heterogeneous piezoelectric solid and certain averages of the electroelastic fields. We proceed by considering a variation of $Z^{\mathrm{T}}_{Mn}(\mathbf{x})$ while $F_{JimN}(\mathbf{x})$ is held unchanged:

$$Z^{\mathrm{T}}_{Mn}(\mathbf{x}) \to Z^{\mathrm{T}}_{Mn}(\mathbf{x}) + \delta Z^{\mathrm{T}}_{Mn}(\mathbf{x}). \tag{29}$$

This implies the corresponding variations of the internal fields:

$$\Sigma_{iJ}(\mathbf{x}) \to \Sigma_{iJ}(\mathbf{x}) + \delta\Sigma_{iJ}(\mathbf{x}), \quad Z_{Mn}(\mathbf{x}) \to Z_{Mn}(\mathbf{x}) + \delta Z_{Mn}(\mathbf{x}). \tag{30}$$

From the non-random boundary conditions we have $\langle \delta\Sigma_{iJ}(\mathbf{x})\rangle = 0$. Taking the variation of Eq. (25), and utilizing the Hill condition (14), we obtain:

$$\begin{aligned}
\Sigma^0_{iJ}\delta Z^*_{Ji}\,|_F &= \langle \Sigma^{\mathrm{I}}_{iJ}\delta Z^{\mathrm{T}}_{Ji}\rangle + \langle \delta\Sigma^{\mathrm{I}}_{iJ} Z^{\mathrm{T}}_{Ji}\rangle \\
&= \langle \Sigma^{\mathrm{I}}_{iJ}\delta Z^{\mathrm{T}}_{Ji}\rangle + \langle \delta\Sigma^{\mathrm{I}}_{iJ} Z^{\mathrm{II}}_{Ji}\rangle - \langle \delta\Sigma^{\mathrm{I}}_{iJ}(Z^{\mathrm{II}}_{Ji} - Z^{\mathrm{T}}_{Ji})\rangle \\
&= \langle \Sigma^{\mathrm{I}}_{iJ}\delta\Sigma^{\mathrm{T}}_{Ji}\rangle + \langle \delta\Sigma^{\mathrm{I}}_{iJ} Z^{\mathrm{II}}_{Ji}\rangle - \langle \delta Z^{\mathrm{I}}_{iJ}\Sigma^{\mathrm{II}}_{Ji}\rangle \\
&= \langle \Sigma^{\mathrm{I}}_{iJ}\delta Z^{\mathrm{T}}_{Ji}\rangle.
\end{aligned} \tag{31}$$

Here $|_F$ denotes that the computation is carried out at constant values of F_{JimN}. In a similar manner, taking variations of Eq. (28) yields:

$$\begin{aligned}
-2\delta H^{\mathrm{II}}\,|_F &= \langle \Sigma^{\mathrm{II}}_{iJ}\delta Z^{\mathrm{T}}_{Ji}\rangle + \langle \delta\Sigma^{\mathrm{II}}_{iJ} Z^{\mathrm{T}}_{Ji}\rangle \\
&= \langle \Sigma^{\mathrm{II}}_{iJ}\delta Z^{\mathrm{T}}_{Ji}\rangle + \langle \delta\Sigma^{\mathrm{II}}_{iJ} Z^{\mathrm{II}}_{Ji}\rangle - \langle \delta\Sigma^{\mathrm{II}}_{iJ}(Z^{\mathrm{II}}_{Ji} - Z^{\mathrm{T}}_{Ji})\rangle \\
&= \langle \Sigma^{\mathrm{II}}_{iJ}\delta Z^{\mathrm{T}}_{Ji}\rangle - \langle \delta(Z^{\mathrm{II}}_{Ji} - Z^{\mathrm{T}}_{Ji})\Sigma^{\mathrm{II}}_{iJ}\rangle \\
&= \langle \Sigma^{\mathrm{II}}_{iJ}\delta Z^{\mathrm{T}}_{Ji}\rangle + \langle \delta Z^{\mathrm{T}}_{Ji}\Sigma^{\mathrm{II}}_{iJ}\rangle.
\end{aligned} \tag{32}$$

Eqs. (31) and (32) can be used to compute mean values of the loading and residual fields if the variation of effective eigenfield and the residual enthalpy are known.

3.5. Second order moments of the electroelastic fields

Here we proceed by considering a variation of $F_{JimN}(\mathbf{x})$ while $Z^{\mathrm{T}}_{Mn}(\mathbf{x})$ is held unchanged:

$$F_{JimN}(\mathbf{x}) \to F_{JimN}(\mathbf{x}) + \delta F_{JimN}(\mathbf{x}). \tag{33}$$

Taking the variation of (27) yields:

$$\begin{aligned}
\delta H^{\mathrm{I}}\,|_{Z^{\mathrm{T}}} &= \frac{1}{2}\langle \Sigma^{\mathrm{I}}_{iJ}\delta F_{JimN}\Sigma^{\mathrm{I}}_{mN}\rangle + \langle \delta\Sigma^{\mathrm{I}}_{iJ} F_{JimN}\Sigma^{\mathrm{I}}_{mN}\rangle \\
&= \frac{1}{2}\langle \Sigma^{\mathrm{I}}_{iJ}\delta F_{JimN}\Sigma^{\mathrm{I}}_{mN}\rangle + \langle \delta\Sigma^{\mathrm{I}}_{iJ} Z^{\mathrm{I}}_{Ji}\rangle \\
&= \frac{1}{2}\langle \Sigma^{\mathrm{I}}_{iJ}\delta F_{JimN}\Sigma^{\mathrm{I}}_{mN}\rangle.
\end{aligned} \tag{34}$$

Here $|_{Z^{\mathrm{T}}}$ signifies that the computation is carried out at constant values of Z^{T}_{Mn}. In a similar manner, taking the variation of Eq. (28) yields:

$$\begin{aligned}\delta H^{\mathrm{II}}\,|_{Z^{\mathrm{T}}} &= \frac{1}{2}\langle \Sigma^{\mathrm{II}}_{iJ}\delta F_{JimN}\Sigma^{\mathrm{II}}_{mN}\rangle + \langle \delta\Sigma^{\mathrm{II}}_{iJ}F_{JimN}\Sigma^{\mathrm{II}}_{mN}\rangle \\ &= \frac{1}{2}\langle \Sigma^{\mathrm{II}}_{iJ}\delta F_{JimN}\Sigma^{\mathrm{II}}_{mN}\rangle + \langle \delta\Sigma^{\mathrm{II}}_{iJ}Z^{\mathrm{II}}_{Ji}\rangle - \langle \delta\Sigma^{\mathrm{II}}_{iJ}Z^{\mathrm{T}}_{Ji}\rangle \\ &= -\frac{1}{2}\langle \Sigma^{\mathrm{II}}_{iJ}\delta F_{JimN}\Sigma^{\mathrm{II}}_{mN}\rangle. \end{aligned} \tag{35}$$

The last right-hand side of Eq. (35) follows from Eq. (28). Eqs. (34) and (35) can be evaluated to obtain second order moments of loading and residual fields, respectively.

The interaction of the loading and residual fields can be obtained by taking a variation of Eq. (22):

$$\langle \delta\Sigma^{\mathrm{I}}_{iJ}F_{JimN}\Sigma^{\mathrm{II}}_{mN}\rangle + \langle \Sigma^{\mathrm{I}}_{iJ}\delta F_{JimN}\Sigma^{\mathrm{II}}_{mN}\rangle + \langle \Sigma^{\mathrm{I}}_{iJ}F_{JimN}\delta\Sigma^{\mathrm{II}}_{mN}\rangle = 0 \tag{36}$$

which yields

$$\begin{aligned}\langle \Sigma^{\mathrm{I}}_{iJ}\delta F_{JimN}\Sigma^{\mathrm{II}}_{mN}\rangle &= -\langle \delta\Sigma^{\mathrm{I}}_{iJ}F_{JimN}\Sigma^{\mathrm{II}}_{mN}\rangle \\ &= -\langle \delta\Sigma^{\mathrm{I}}_{iJ}Z^{\mathrm{II}}_{Ji}\rangle + \langle \delta\Sigma^{\mathrm{I}}_{iJ}Z^{\mathrm{T}}_{Ji}\rangle \\ &= \Sigma^{0}_{iJ}\delta Z^{*}_{Ji}\,|_{Z^{\mathrm{T}}}\,. \end{aligned} \tag{37}$$

4. Application to matrix-based piezoelectric composites

The only assumption made in the derivation thus far is that of statistical homogeneity. Otherwise we have retained complete generality concerning the details of the heterogeneous microstructure. In order to make further progress we must, at least to some degree, specify the heterogeneous microstructure. Here we apply the general theory to a matrix-based composite consisting of n phases, and then further specialize those results to a two-phase composite. We note that the general results can also be applied to a piezoelectric polycrystal where we regard grains of different orientations as different phases, but those results will be presented elsewhere.

4.1. Multiphase matrix-based composites

We consider a composite consisting of a matrix (phase 1) containing $n-1$ dispersed phases. As a result, the material properties $F_{JimN}(\mathbf{x})$ and $Z^{\mathrm{T}}{}_{Mn}(\mathbf{x})$ take on the values $F_{JimN}|_r$ and $Z^{\mathrm{T}}_{Mn}|_r (r = 1-n)$ with probabilities c_r. Here $|_r$ is used to denote the property of a variable in phase r. We typically call c_r the volume fraction and it satisfies

$$\sum_{r=1}^{n} c_r = 1.$$

The material properties can thus be written as:

$$F_{JimN}(\mathbf{x}) = \sum_{r=1}^{n} F_{JimN}\,|_r\,\Theta_r(\mathbf{x}),$$
$$Z^{\mathrm{T}}_{Mn}(\mathbf{x}) = \sum_{r=1}^{n} Z^{\mathrm{T}}_{Mn}\,|_r\,\Theta_r(\mathbf{x}). \tag{38}$$

In Eq. (38) the characteristic function Θ_r describes the topology of the microstructure, i.e.

$$\Theta_r(\mathbf{x}) = \begin{cases} 1 & \text{if} \quad \mathbf{x} \in r, \\ 0 & \text{if} \quad \mathbf{x} \notin r. \end{cases} \tag{39}$$

Note the following relation regarding any property $A(x)$ that varies over the microstructure:

$$\langle A(x)\Theta_r(\mathbf{x})\rangle = c_r\langle A(\mathbf{x})\,|_r\rangle. \tag{40}$$

Now, consider a special variation of the compliance and eigenfield where the material properties of phase r change by $\delta F_{JimN}\big|_r$ and $\delta Z^{\mathrm{T}}_{Mn}\big|_r$, while the topology and material constants of the other phases remain unchanged:

$$\delta F_{JimN} = \delta F_{JimN}\,|_r\,\Theta_r(\mathbf{x}),$$
$$\delta Z^{\mathrm{T}}_{Mn} = \delta Z^{\mathrm{T}}_{Mn}\,|_r\,\Theta_r(\mathbf{x}). \tag{41}$$

In Eq. (41), r ranges from 1 to n and no sum over r is implied. Applying these variations to Eqs. (31), (32), (34), (35) and (37), and using (40) yields:

$$\langle \Sigma^{\mathrm{I}}_{iJ}\,|_r\rangle \delta Z^{\mathrm{T}}_{Ji} = \frac{1}{c_r}\Sigma^0_{iJ}\delta Z^*_{Ji}\,|_F, \tag{42}$$

$$\langle \Sigma^{\mathrm{II}}_{iJ}\,|_r\rangle \delta Z^{\mathrm{T}}_{Ji} = -\frac{1}{c_r}\delta H^{\mathrm{II}}\,|_F, \tag{43}$$

$$\langle \Sigma^{\mathrm{I}}_{iJ}\Sigma^{\mathrm{I}}_{mN}\,|_r\rangle \delta F_{JimN}\,|_r = \frac{2}{c_r}\delta H^{\mathrm{I}}\,|_{Z^{\mathrm{T}}}, \tag{44}$$

$$\langle \Sigma^{\mathrm{II}}_{iJ}\Sigma^{\mathrm{II}}_{mN}\,|_r\rangle \delta F_{JimN}\,|_r = -\frac{2}{c_r}\delta H^{\mathrm{II}}\,|_{Z^{\mathrm{T}}}, \tag{45}$$

$$\langle \Sigma^{\mathrm{I}}_{iJ}\Sigma^{\mathrm{II}}_{mN}\,|_r\rangle \delta F_{JimN}\,|_r = \Sigma^0_{iJ}\delta Z^*_{Ji}\,|_{Z^{\mathrm{T}}}\ . \tag{46}$$

Eqs. (42)–(46) establish the rigorous connections between first and second order moments of the field variables, and variations of the effective properties.

4.2. Two-phase matrix-based composites

Here we specialize the results of the previous section to a composite consisting of a matrix with a single embedded phase. We require that the material properties of the dispersed phase

are constant with respect to a fixed sample coordinate system. Thus orientational variations of an anisotropic dispersed phase are prohibited. The two phases are characterized by their volume fractions c_1 and c_2, compliance tensors $F_{JimN}|_1$ and $F_{JimN}|_2$, and eigenfields $Z^{\mathrm{T}}_{Mn}|_1$ and $Z^{\mathrm{T}}_{Mn}|_2$. As a result, in the sample-fixed coordinated system $F_{JimN}(\mathbf{x})$ and $Z^{\mathrm{T}}_{Mn}(\mathbf{x})$ can assume only two values.

The average field $\langle \Sigma_{cD} \rangle$ in the composite is equal to the volume-weighted average of Σ_{cD} over each phase. In addition, it is also equal to the external load Σ^0_{cD}. As a result we have $c_1\langle \Sigma^{\mathrm{I}}_{cD}|_1 \rangle + c_2\langle \Sigma^{\mathrm{I}}_{cD}|_2 \rangle = \Sigma^0_{\mathrm{cD}}$. Applying an analogous result for $\langle Z_{Ab} \rangle$, and using the constitutive equations for the phases and the composite yields:

$$c_1 F_{AbcD}\,|_1\,\langle \Sigma^{\mathrm{I}}_{cD}\,|_1\rangle + c_2 F_{AbcD}\,|_2\,\langle \Sigma^{\mathrm{I}}_{cD}\,|_2\rangle = F^*_{AbcD}\Sigma^0_{cD}. \tag{47}$$

Provided that $(F_{JimN}|_1 - F_{JimN}|_2)^{-1}$ exists, Eq. (47) may be solved to yield

$$\begin{aligned}
\langle \Sigma^{\mathrm{I}}_{cD}\,|_1\rangle &= \frac{1}{c_1}(F_{AbcD}\,|_1 - F_{AbcD}\,|_2)^{-1}(F^*_{AbiJ} - F_{AbiJ}\,|_2)\Sigma^0_{iJ},\\
\langle \Sigma^{\mathrm{I}}_{cD}\,|_2\rangle &= \frac{1}{c_2}(F_{AbcD}\,|_2 - F_{AbcD}\,|_1)^{-1}(F^*_{AbiJ} - F_{AbiJ}\,|_1)\Sigma^0_{iJ}.
\end{aligned} \tag{48}$$

In an analogous manner we obtain:

$$\begin{aligned}
\langle \Sigma^{\mathrm{II}}_{cD}\,|_1\rangle &= \frac{1}{c_1}(F_{AbcD}\,|_1 - F_{AbcD}\,|_2)^{-1}(Z^*_{Ab} - \overline{Z^{\mathrm{T}}_{Ab}})\\
\langle \Sigma^{\mathrm{II}}_{cD}\,|_2\rangle &= \frac{1}{c_2}(F_{AbcD}\,|_2 - F_{AbcD}\,|_1)^{-1}(Z^*_{Ab} - \overline{Z^{\mathrm{T}}_{Ab}})
\end{aligned} \tag{49}$$

where $\overline{Z^{\mathrm{T}}_{Ab}} = c_1 Z^{\mathrm{T}}_{\mathrm{Ab}}|_1 + c_2 Z^{\mathrm{T}}_{Ab}|_2$.

Upon substituting Eq. (48) into Eq. (25), after some manipulation, we obtain:

$$Z^*_{Ji} = \overline{Z^{\mathrm{T}}_{Ji}} + (\overline{F_{AbiJ}} - F^*_{AbiJ})(F_{AbmN}\,|_1 - F_{AbmN}\,|_2)^{-1}(Z^{\mathrm{T}}_{Nm}\,|_2 - Z^{\mathrm{T}}_{Nm}\,|_1) \tag{50}$$

where $\overline{F_{AbiJ}} = c_1 F_{AbiJ}|_1 + c_2 F_{AbiJ}|_2$. Eq. (50) is an exact result that rigorously connects the effective eigenfield to the effective electroelastic moduli. A similar equation for heterogeneous elastic solids was first obtained by Rosen and Hashin [36]. For heterogeneous piezoelectric solids, Dunn [15] and Benveniste [3] derived analogous results via two different approaches. We note that Benveniste obtained even more general results for multiphase media.

Substituting Eq. (49) into Eq. (28), we can express the stored enthalpy as:

$$H^{\mathrm{II}} = \frac{1}{2}(Z^{\mathrm{T}}_{Ji}\,|_2 - Z^{\mathrm{T}}_{Ji}\,|_1)(F_{AbiJ}\,|_1 - F_{AbiJ}\,|_2)^{-1}(Z^*_{Ab} - \overline{Z^{\mathrm{T}}_{Ab}}). \tag{51}$$

It is apparent that H^{II} can be expressed in terms only of the effective electroelastic moduli of the composite and the properties of two phases. As such, it can also be considered an effective material property. Note that in the derivation, no specific microstructure was assumed. These exact relations are thus applicable to two-phase composites with a wide range of microstructural geometries. Also note that we have not specified how one obtains the effective electroelastic moduli of the composite, but have simply assumed that they can be obtained. This may be done either experimentally or through detailed micromechanical modeling.

Table 1. Electroelastic moduli of the PZT-5 fibers and the polymer matrix. The units of C_{ij} are GPa, e_{ij} are C/m^2, Δ_{ij} are $\times 10^{-6}$/K, and γ_3 is $\times 10^5$ N/CK

	C_{11}	C_{12}	C_{13}	C_{33}	C_{44}	e_{31}	e_{33}	e_{15}	$^*\kappa_{11}\kappa_0$	$^*\kappa_{33}/_0$	Δ_{11}	Δ_{33}	γ_3
PZT-5	121.0	75.4	75.2	111.0	21.1	−5.4	15.8	12.3	916.0	830.0	−3.2	14.9	−0.332
Polymer	8.03	4.32	4.32	8.03	1.85	0.0	0.0	0.0	4.0	4.0	60.0	60.0	0.0

$^*\kappa_0 = 8.85 \times 10^{-12}$/C^2/Nm^2 = permittivity of free space.

5. Numerical results for two-phase composites

In this section we demonstrate the applicability of the theory by applying it to a two-phase composite consisting of continuous PZT-5 piezoelectric fibers embedded in a polymer matrix. The electroelastic moduli of the two phases are presented in Table 1. The x_3-direction is aligned with the fiber axis and the x_1–x_2 plane is isotropic, both for the transversely isotropic fibers and the composite as a whole. Calculations were carried out for three different types of external loading: electrical loading along the x_3-direction, hydrostatic pressure loading, and a uniform temperature change. These correspond to typical loading environments when a piezoelectric composite is used in a transducer application, for example, as a hydrophone. The results for the thermal loading are not shown because they are qualitatively similar to those for a hydrostatic pressure loading. The calculation procedure, which has been implemented into a FORTRAN computer code, is outlined in Table 2.

The estimation of the effective electroelastic moduli of the composite in step 2 deserves more discussion. In principle, the effective electroelastic moduli can be estimated by theory or measured experimentally. Of course, the estimates of the internal fields can only be expected to be as accurate as the model used to predict the effective moduli or the measurements of the effective moduli. In order to demonstrate the application of the theory, we have used three different micromechanics theories to predict the effective moduli: the Mori–Tanaka, the self-

Table 2. Outline of calculation procedure for average fields and field fluctuations

1. Input electroelastic properties and volume fractions of the fibers and matrix, and the applied loads.
2. Compute the effective electroelastic moduli of the composite using a micromechanics model.
3. Compute the effective thermal properties and the stored enthalpy density using (50), (51), and (27).
4. Compute the average fields using (48) and (49).
5. Keep all components of the electroelastic moduli of one phase constant except one, E_{iJKl}, which is changed by the amount $\pm\Delta E_{iJKl}$. Repeat steps 2 and 3 and then calculate

$$\Delta H_{iJKl} = \frac{H(E_{iJKl} + \Delta E_{iJKl}) - H(E_{iJKl} - \Delta E_{iJKl})}{2} \quad \text{and} \quad \langle \Sigma_{iJ}\Sigma_{Kl}\rangle = \frac{\Delta H_{iJKl}}{\Delta E_{iJKl}} \text{ (no summation assumed here).}$$

6. Decrease ΔE_{iJKl} and repeat step 5 until converge is obtained. The second order moments are then computed using (42)–(46).
7. Compute variations of the internal fields from $\Delta\Sigma_{iJ} = \sqrt{\langle \Sigma_{iJ}\Sigma_{iJ}\rangle - \langle \Sigma_{iJ}\rangle\langle \Sigma_{iJ}\rangle}$.

consistent, and the differential theories. Over the past few years these approaches have become reasonably well-known in the micromechanics community (see for example Refs [32, 33] for extensive details and numerous applications). Their inner workings will not be discussed here, except as is appropriate in the interpretation of the predicted internal fields. The interested reader is referred to Ref. [22] for details regarding the three micromechanics theories as applied to piezoelectric composites. In addition, the strengths and weaknesses of each of the approaches is not the focus of this work, and so will not be discussed in detail either, but again only as is appropriate in the interpretation of the predicted internal fields.

To our knowledge, no previous work has been published regarding modeling of internal fields in heterogeneous piezoelectric solids. Thus, in order to validate our results, we applied it to the extreme cases of uncoupled elastostatic and electrostatic behavior of heterogeneous solids. Specifically, we used the self consistent method to calculate the uncoupled elastic and dielectric constants for a two-phase composite consisting of spherical particles embedded in a matrix. We used the input data of Bobeth and Diener [9] for both the elastic and electric properties for the composite constituents. We then computed the average fields and the field fluctuations in the manner described above. Our numerical results agreed with those of Bobeth and Diener [9] for both the elastic and electric average internal fields and fluctuations. We also used the Mori–Tanaka theory to perform the same calculations and found general agreement with the self-consistent method for the predicted internal fields, but we found the Mori–Tanaka theory resulted in predictions of no field fluctuations. This was also the case with regard to the coupled field behavior of the piezoelectric composites with continuous fibers. This is in agreement with the results of Kreher and Pompe [30] for the elastic fields in a composite with spherical inhomogeneities. Here we adopt the terminology of Mura [32] where, by inhomogeneity we mean a subdomain in a matrix that has different elastic constants than the matrix, and by inclusion we mean a subdomain with the same elastic constants as the matrix, but with an eigenstrain. In light of this, in the calculations of average fields and field fluctuations that are presented below, we use only the self-consistent scheme because the Mori–Tanaka method predicts no internal field fluctuations (and thus is not suitable for modeling field fluctuations). The selection of the self-consistent scheme is in spite of the fact that it has received considerable criticism for its applicability to the prediction of effective moduli of matrix-based composites. We do not claim that this is the best micromechanics model for this purpose, but we simply use it to demonstrate the applicability of the rigorous theory of internal fields and fluctuations proposed here. For completeness, in the Appendix we briefly review the application of the self-consistent method and also the solution for the key auxiliary problem: the solution for a single piezoelectric inhomogeneity in an infinite matrix. The latter auxiliary problem is solved using Eshelby's equivalent inclusion method [32, 41]. In the solution of the auxiliary problem, we take advantage of the uniformity of the electroelastic fields in the inhomogeneity which trivializes the required averaging for the micromechanics model.

Figures 1–3 show the average stresses, $\langle\sigma_{11}\rangle$ and $\langle\sigma_{33}\rangle$, and the average electric displacement, $\langle D_3\rangle$, along with their variations in each phase of the PZT-5/polymer composite. Regarding the transverse stresses, our discussion will focus on $\langle\sigma_{11}\rangle$, but we remind that $\langle\sigma_{11}\rangle = \langle\sigma_{22}\rangle$ due to the transversely isotropic symmetry of the composite. Several interesting phenomena are present and these deserve discussion.

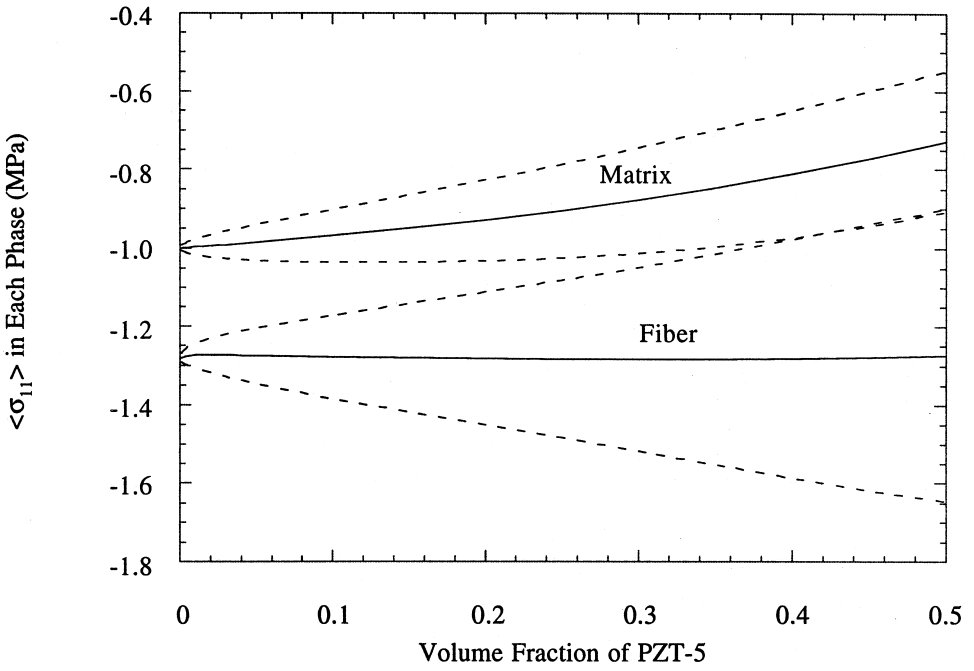

Fig. 1. Average stress $\langle \sigma_{11} \rangle$ in a continuous PZT-5 fiber reinforced polymer composite due to an applied hydrostatic pressure of 1 MPa, vs. the volume fraction of PZT-5. The solid line is $\langle \sigma_{11} \rangle = \langle \sigma_{22} \rangle$ and the broken line is $\langle \sigma_{11} \rangle \pm \Delta\sigma_{11}$.

Under hydrostatic loading, stresses in the composite can be thought of as arising from two sources: the applied axial stress, σ_{33}^0, and the applied in-plane stresses, σ_{11}^0 and σ_{22}^0. For σ_{33}^0, the axial strain in the fiber is equal to that in the matrix. Because the fiber is much stiffer than the matrix, $\langle \sigma_{33} \rangle$ in the fiber is much larger than that in the matrix, which differs little from σ_{33}^0 at low fiber volume fractions. Thus, at low volume fractions, $\langle \sigma_{33} \rangle$ in the fibers is much higher than σ_{33}^0. The applied σ_{11}^0 and σ_{22}^0 cause tensile stress in the fibers in the x_3 direction due to the fact that the fiber and matrix constrain each other in the x_3 direction, and the polymer matrix wants to extend more in the x_3 direction because it is more compliant than the matrix. However, this tensile stress is smaller than the compressive stress in the x_3 direction caused by σ_{33}^0 and so the total axial stress in the fiber is compressive. A similar argument shows that $\langle \sigma_{11} \rangle$ in the fibers is only slightly larger than the applied $\sigma_{11}^0 = \sigma_{22}^0$. The major contributor to $\langle \sigma_{11} \rangle$ is the applied $\sigma_{11}^0 = \sigma_{22}^0$. The applied compressive stress σ_{33}^0 induces a tensile stress in fibers in the x_1 direction, but it is a small second order effect caused by the difference in Poisson ratios between the fibers and the matrix.

The discussion of these elastic effects sets the stage for the discussion of some interesting effects that arise due to piezoelectricity. Specifically, the stresses in the fibers, especially $\langle \sigma_{33} \rangle$, will cause an electric field $\langle E_3 \rangle$ in the fibers due to the piezoelectric effect. Because the stresses in the fiber are higher than they would be in a homogeneous piezoelectric under the same far-field hydrostatic load, the electric field in the fibers will be higher than it would in a

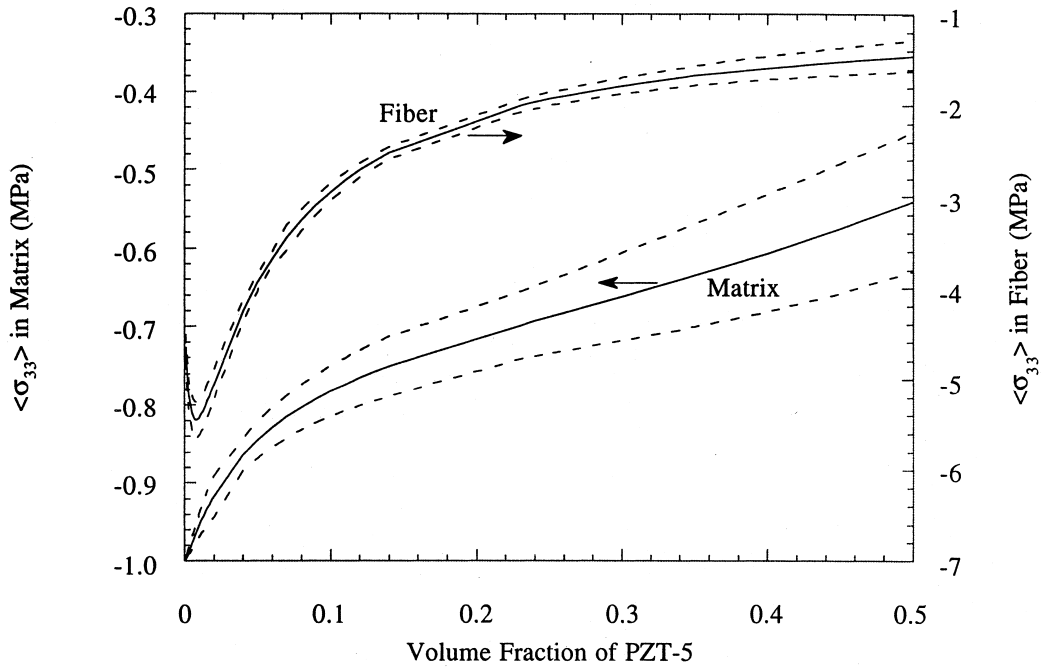

Fig. 2. Average stress $\langle\sigma_{33}\rangle$ in a continuous PZT-5 fiber reinforced polymer composite due to an applied hydrostatic pressure of 1 MPa, vs. the volume fraction of PZT-5. The solid line is $\langle\sigma_{33}\rangle$ and the broken line is $\langle\sigma_{33}\rangle \pm \Delta\sigma_{33}$.

homogeneous piezoelectric. Now, the electric field is uniform in the x_3 direction, and because it is irrotational, it also can not vary in the x_1 and x_2 directions. Thus, the electric field in the x_3 direction caused by the hydrostatic load is uniform throughout the composite.

For a specified hydrostatic load, $\langle E_3\rangle = 0$ at a volume fraction of zero because the polymer matrix is not piezoelectric. It also takes on another value at a volume fraction of unity that corresponds to the homogeneous piezoelectric. Somewhere in between, $\langle E_3\rangle$ in the fibers is higher than that in the corresponding homogeneous piezoelectric because $\langle\sigma_{33}\rangle$ in fibers is higher than it would be in a homogeneous piezoelectric, and thus reaches a maximum value at a volume fraction somewhere between zero and unity. This value turns out to be at a volume fraction of about 0.006.

The hydrostatic load causes tensile strain in the x_1 and x_2 directions, and compressive strain in the x_3 direction in the fibers at low volume fractions. This is because $\langle\sigma_{33}\rangle$ is much larger than $\langle\sigma_{11}\rangle$ at low volume fractions, so that the magnitude of $\langle\varepsilon_{11}\rangle$ caused by the Poisson effect is larger than that caused by $\langle\sigma_{11}\rangle$ (because $\langle\sigma_{33}\rangle$ is about four times larger than $\langle\sigma_{11}\rangle$ in the fibers at low volume fractions, while Poisson ratio is about 0.3, and $\langle\sigma_{22}\rangle$ will also cause a tensile strain $\langle\varepsilon_{11}\rangle$). As a result, the hydrostatic strain $\langle\varepsilon_h\rangle = 2\langle\varepsilon_{11}\rangle + \langle\varepsilon_{33}\rangle$ in the fibers is compressive at low volume fractions. Both the compressive $\langle\varepsilon_{33}\rangle$ and the tensile $\langle\varepsilon_{11}\rangle$ decrease quickly, but monotonically, with an increase in the fiber volume fraction. However, because $\langle\varepsilon_{11}\rangle$ decreases faster than $\langle\varepsilon_{33}\rangle$, and they are of opposite sign, there exists a peak in $\langle\varepsilon_h\rangle$. Now

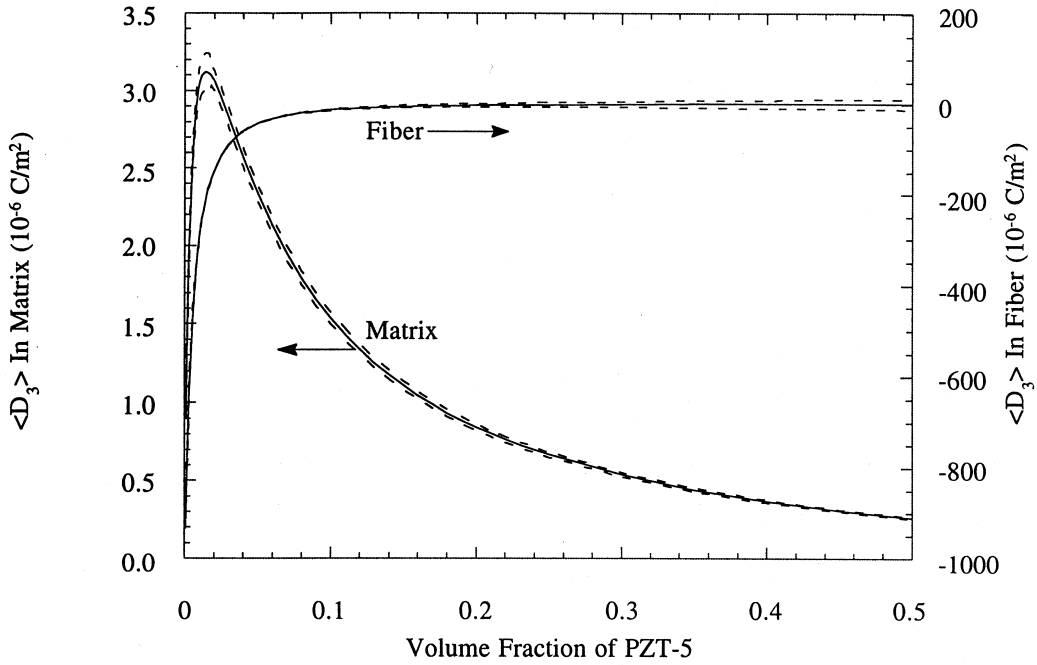

Fig. 3. Average electric displacement $\langle D_3 \rangle$ in a continuous PZT-5 fiber reinforced polymer composite due to an applied hydrostatic pressure of 1 MPa, vs. the volume fraction of PZT-5. The solid line is $\langle D_3 \rangle$ and the broken line is $\langle D_3 \rangle \pm \Delta D_3$.

there exists a peak in $\langle E_3 \rangle$ and $\langle \varepsilon_h \rangle$ in the fiber phase. For $\langle \sigma_{33} \rangle$ in the fibers, the components related to $\langle E_3 \rangle$ and $\langle \varepsilon_h \rangle$ are of the same sign. This leads to a peak in $\langle \sigma_{33} \rangle$ in the fibers. Because the polymer matrix does not exhibit piezoelectricity, there is no peak in the stress in the matrix, but because there is a peak in $\langle E_3 \rangle$, there is a peak in $\langle D_3 \rangle$ in the matrix.

Fig. 4 shows the average stress $\langle \sigma_{33} \rangle$ in the matrix and fibers caused by an applied electric displacement D_3^0. $\langle \sigma_{33} \rangle$ in the fibers is very high at low volume fractions, and drops very fast as the fiber volume fraction increases. There is a peak in $\langle \sigma_{33} \rangle$ in the matrix at a low fiber volume fraction. The high stress in the fiber at low volume fractions arises because the applied electrical displacement is consumed by the small amount of fibers, and thus the electric displacement is large which then leads to lazrge stresses in the fiber. As the fiber volume fraction increases, the applied electric displacement is shared by more and more fibers and this causes the stress in the fibers to decrease. The peak in $\langle \sigma_{33} \rangle$ in the matrix is due to the fact that at zero fiber volume fraction, the stress in the matrix is zero. As the fiber volume fraction increases, the composite becomes piezoelectric, and the applied electric displacement causes stress and strain in the fibers. This induces stress in the matrix to cancel the stress in the fibers to maintain self equilibrium. As the fiber volume fraction increases, the stress in the fibers decreases rapidly, causing the stress in the matrix to also decrease, thus resulting in a peak in the stress in the matrix.

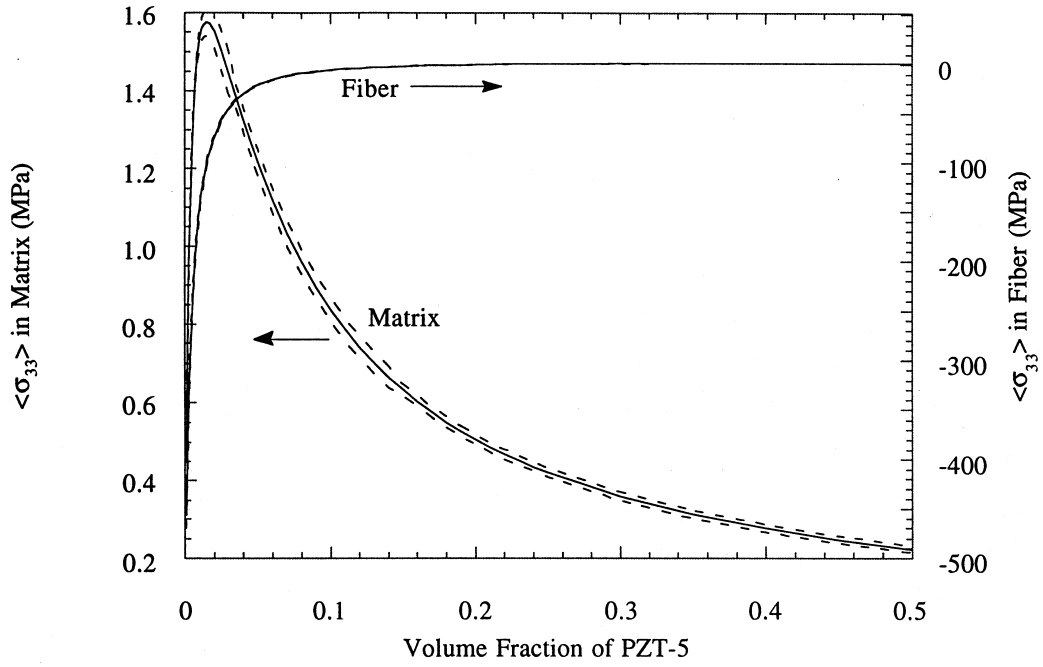

Fig. 4. Average stress $\langle\sigma_{33}\rangle$ in a continuous PZT-5 fiber reinforced polymer composite due to an applied electric displacement of 0.001 C/m^2 in the x_3-direction, vs. the volume fraction of PZT-5. The solid line is $\langle\sigma_{33}\rangle$ and the broken line is $\langle\sigma_{33}\rangle \pm \Delta\sigma_{33}$.

From Figs. 1–4, it is clear that there are no field variations at zero fiber volume fraction, as expected. With the addition of fibers to the polymer matrix, variations in the fields are observed. This is because increased uncertainty exists in both the geometrical arrangement of the fibers in the matrix, and in the details of the interaction between the fibers. These two phenomena are reflected by the increase in field variations in both phases as the fiber volume fraction increases. Interestingly, the field variations tend to reach a maximum at the points where the average fields peak. We also see that, due to the uniform fibrous configuration of the composite in the x_3 direction, the field variations are higher in the x_1 and x_2 directions than those in the x_3 direction.

6. Conclusion

A theory, applicable to both polycrystalline ceramics as well as matrix-based composites, was developed to analyze the internal fields in heterogeneous piezoelectric solids. It was used to derive expressions for mean values and variations of the internal fields due to external loading and eigenfields. The theory was applied to multiphase matrix-based piezoelectric composites, and explicit relations were obtained for two-phase composites. Exact connections were established between the effective thermal properties and the effective electroelastic moduli for

two-phase composites. These agree with previous results of Benveniste [3] and Dunn [15] obtained by two different approaches. Also, we expressed the stored enthalpy of the heterogeneous solid as an explicit function of the effective thermoelectroelastic properties. To demonstrate the applicability of the theory, numerical results for average fields and field variations were presented for a two-phase composite consisting of continuous piezoelectric fibers embedded in a polymer matrix.

Appendix A

A.1. Micromechanics model and auxiliary single inhomogeneity problem

The effective electroelastic moduli E^*_{iJMn} of a two-phase composite consisting of perfectly-bonded piezoelectric phases can be expressed as [21, 22]:

$$E^*_{iJMn} = E_{iJMn}\,|_1 + c_2(E_{iJAb}\,|_2 - E_{iJAb}\,|_1)A_{AbMn}. \tag{A1}$$

In equation (A1) A_{AbMn} is the concentration tensor that, due to linearity, relates the average strain and potential gradients in phase 2 to that in the composite (which are equal to those applied under displacement boundary conditions, Z^0_{Ab}), i.e.

$$\langle Z_{Mn}\,|_2\rangle = A_{MnAb}Z^0_{Ab}. \tag{A2}$$

The estimation of A_{MnAb} is thus the key to predicting the effective moduli E^*_{iJMn}. It is well-known that numerous models exist that can be used to estimate the concentration factor at this point, each with their advantages and disadvantages. For the reasons discussed in Section 5, we use the self-consistent method. In simplest terms, this amounts to assuming:

$$A_{MnAb} = [I_{MnAb} + S_{MnLk}E^{*-1}_{LkiJ}(E_{iJAb}\,|_2 - E^*_{iJAb})]^{-1}. \tag{A3}$$

Here I_{MnAb} is a collection of fourth- and second-rank identity tensors and the superscript -1 denotes an inversion operation. A_{MnAb} is recognized to be the dilute concentration factor which is obtained from the solution of the auxiliary problem of a single inhomogeneity embedded in an infinite matrix with electroelastic moduli equal to the effective moduli of the composite E^*_{LkiJ}. In equation (A4), S_{MnLk} are the electroelastic Eshelby tensors and have been defined by Dunn and Taya [21, 22]. S_{MnLk}, and of course A_{MnAb}, are most easily obtained by using the equivalent inclusion method [32, 41] as applied to piezoelectric inclusions and inhomogeneities. For ellipsoidal inclusions, are functions of the shape of the inclusion and the electroelastic moduli of the matrix. Furthermore, in this case the electroelastic fields in the inclusion (or inhomogeneity) are uniform when a uniform far-field loading is applied. General expressions for S_{MnLk} in terms of a surface integral over the unit sphere are given by Dunn and Taya [21] for ellipsoidal inclusions in generally anisotropic piezoelectric solids. Explicit expressions for S_{MnLk} for spheroidal inclusions in a transversely isotropic piezoelectric solid are given in Ref. [24]. For elliptical cylindrical inclusions in a transversely isotropic solid, such as those considered here, the solution is greatly simplified and the non-zero S_{MnLk} reduce to:

$$
\begin{aligned}
S_{1111} &= \frac{[(3+2\alpha)C_{11}+C_{12}]\alpha}{2(1+\alpha)^2 C_{11}} \\
S_{1122} &= \frac{[(1+2\alpha)C_{12}-C_{11}]\alpha}{2(1+\alpha)^2 C_{11}} \\
S_{1133} &= \frac{\alpha C_{13}}{(1+\alpha)C_{11}} \\
S_{2211} &= \frac{(2+1\alpha)C_{12}-\alpha C_{11}}{2(1+\alpha)^2 C_{11}} \\
S_{2222} &= \frac{(2+3\alpha)C_{11}+\alpha C_{12}}{2(1+\alpha)^2 C_{11}} \\
S_{2233} &= \frac{C_{13}}{(1+\alpha)C_{11}} \\
S_{2323} &= S_{2332} = S_{3223} = S_{3232} = \frac{1}{2(1+\alpha)} \\
S_{1313} &= S_{1331} = S_{3113} = S_{3131} = \frac{\alpha}{2(1+\alpha)} \\
S_{1212} &= S_{1221} = S_{2112} = S_{2121} = \frac{(1+\alpha+\alpha^2)C_{11}-\alpha C_{12}}{2(1+\alpha)^2 C_{11}} \\
S_{1143} &= \frac{\alpha e_{31}}{(1+\alpha)C_{11}} \\
S_{2243} &= \frac{e_{31}}{1+\alpha C_{11}} \\
S_{4141} &= \frac{\alpha}{1+\alpha} \\
S_{4242} &= \frac{1}{1+\alpha}.
\end{aligned}
\tag{A4}
$$

In equation (A4), $\alpha = a_2/a_1 (a_3 \to \infty)$ denotes the aspect ratio of the elliptical inclusion, a_i ($i = 1$–3) are the inclusion semiaxes, and the well-known Voigt two-index notation has been used for the electroelastic moduli. Note that a circular cylindrical inclusion is obtained when $\alpha = 1$.

References

[1] G. Arlt, Twinning in ferroelectric and ferroelastic ceramics: stress relief, J. Mat. Sci. 25 (1990) 2655–2666.

[2] D.M. Barnett, J. Lothe, Dislocations and line charges in anisotropic piezoelectric insulators, Phys. Stat. Sol. (b) 67 (1975) 105–111.

[3] Y. Benveniste, Universal relations in piezoelectric composites/B with eigenstress and polarization fields I, binary media: local fields and effective behavior, J. Appl. Mech. 60 (1993a) 265–269.

[4] Y. Benveniste, Universal relations in piezoelectric composites with eigenstress and polarization fields II, multi-phase media: effective behavior, J. Appl. Mech. 60 (1993b) 270–275.

[5] Y. Benveniste, Exact results in the micromechanics of fibrous piezoelectric composites exhibiting pyroelectricity, Proc. Royal Soc. London A 441 (1993c) 59–81.
[6] Y. Benveniste, Exact results concerning the local fields and effective properties in piezoelectric composites, ASME J. Engng Mat. Technol. 260 (1994a) 260–267.
[7] Y. Benveniste, On the micromechanics of fibrous piezoelectric composites, Mech. Mat. 18 (1994b) 183–193.
[8] Y. Benveniste, G.J. Dvorak, Uniform fields and universal relations in piezoelectric composites, J. Mech. Phys. Solids 40 (1992) 1295–1312.
[9] M. Bobeth, G. Diener, Field fluctuations in multicomponent mixtures, J. Mech. Phys. Solids 34 (1986) 1–17.
[10] M. Bobeth, G. Diener, Static elastic and thermoelastic field fluctuations in multiphase composites, J. Mech. Phys. Solids 35 (1987) 137–149.
[11] V.A. Buryachenko, W. Kreher, Internal residual stresses in heterogeneous solids—a statistical theory for particulate composites, J. Mech. Phys. Solids 43 (1995) 1105–1125.
[12] H. Cao, Q.M. Zhang, L.E. Cross, Theoretical study on the static performance of piezoelectric ceramic–polymer composites with 1–3 connectivity, J. Appl. Phys. 72 (1992a) 5814–5821.
[13] H. Cao, Q.M. Zhang, L.E. Cross, Theoretical study on the static performance of piezoelectric ceramic–polymer composites with 2–2 connectivity, IEEE Trans. Ultrasonics, Ferroelectrics Freq. Control 40 (1992b) 103–109.
[14] T.Y. Chen, Micromechanical estimates of the overall thermoelectroelastic moduli of multiphase fibrous composites, Int. J. Solids Struct. 31 (1994) 3099–3111.
[15] M.L. Dunn, Exact relations between the thermoelectroelastic moduli of heterogeneous materials, Proc. Royal Soc. London A 441 (1993a) 549–557.
[16] M.L. Dunn, Micromechanics of coupled electroelastic composites: effective thermal expansion and pyroelectric coefficients, J. Appl. Phys. 73 (1993b) 5131–5140.
[17] M.L. Dunn. 1993c. Exact relations between the thermal and electroelastic moduli of composite materials with emphasis on two-phase laminates. in: Varadan VK, (Ed.), Proceedings of the 1993 North American Conference on Smart Structures and Materials: Smart Materials. Albuquerque, NM, USA vol. 1916. pp. 275–285.
[18] M.L. Dunn, Thermally induced fields in electroelastic composite materials: average fields and effective behavior, ASME J. Engng Mat. Technol. 116 (1994) 200–207.
[19] M.L. Dunn, A theoretical framework for the analysis of thermoelectroelastic heterogeneous media with applications, J. Intell. Mat. Systems Struct. 6 (1995a) 255–265.
[20] M.L. Dunn, Effects of grain shape anisotropy, porosity, and microcracks on the elastic and dielectric constants of polycrystalline piezoelectric ceramics, J. Appl. Phys. 78 (1995b) 1533–1542.
[21] M.L. Dunn, M. Taya, An analysis of piezoelectric composite materials containing ellipsoidal inhomogeneities, Proc. Royal Soc. London A 443 (1993a) 265–287.
[22] M.L. Dunn, M. Taya, Micromechanics predictions of the effective electro-elastic moduli of piezoelectric composites, Int. J. Solids Struct. 30 (1993b) 161–175.
[23] M.L. Dunn, M. Taya, Electromechanical properties of porous piezoelectric ceramics, J. Am. Cer. Soc. 76 (1993c) 1697–1706.
[24] M.L. Dunn, H.A. Wienecke, Inclusions and inhomogeneities in transversely isotropic solids, Int. J. Solids Struct. 34 (1997) 3571–3582.
[25] A.A. Grekov, S.O. Kramarov, A.A. Kuprienko, Effective properties of a transversely isotropic piezocomposite with cylindrical inclusions, Ferroelectrics 99 (1989) 115–126.
[26] R. Hill, Elastic properties of reinforced solids: some theoretical principles, J. Mech. Phys. Solids 11 (1963) 357–372.
[27] W. Kreher, Internal stresses and relations between effective thermalelastic properties of stochastic solids—some exact solutions, Z. Angew. Math. Mech. 68 (1988) 147–154.
[28] W. Kreher, Residual stresses and stored elastic energy of composites and polycrystals, J. Mech. Phys. Solids 38 (1990) 115–128.
[29] W. Kreher, A. Molinari, Residual stresses in polycrystals as influenced by grain shape and texture, J. Mech. Phys. Solids 41 (1993) 1955–1977.
[30] W. Kreher, W. Pompe, Internal stresses in heterogeneous solids. Akademie, Berlin, 1989.
[31] F. Kroupa, K. Nejezchleb, I. Saxl, Anisotropy of internal stresses in poled PZT ceramics, Ferroelectrics 88 (1988) 123–137.

[32] T. Mura, Micromechanics of defects in solids. 2nd ed. Martinus Nijhoff, The Hague, 1987.
[33] S. Nemat-Nasser, M. Hori, Micromechanics: overall properties of heterogeneous solids. Elsevier, Amsterdam, 1993.
[34] T. Olson, M. Avellaneda, Effective dielectric and elastic constants of piezoelectric polycrystals, J. Appl. Phys. 71 (1992) 4455–4464.
[35] M. Ortiz, A. Molinari, Microstructural thermal stresses in ceramic materials, J. Mech. Phys. Solids 36 (1988) 385–400.
[36] B.W. Rosen, Z. Hashin, Effective thermal expansion coefficients and specific heats of composite materials, Int. J. Engng Sci. 8 (1970) 157–173.
[37] K. Schulgasser, Relationships between the effective properties of transversely isotropic piezoelectric composites, J. Mech. Phys. Solids 40 (1992) 473–479.
[38] N.R. Sottos, L. Li, W.R. Scott, M.J. Ryan. 1993. Micromechanical behavior of 1–3 piezocomposites. in: Varadan VK, (ed.), Proceedings of the 1993 North American Conference on Smart Structures and Materials: Smart Materials. Society of Photo-optical Instrumentation Engineers, Bellingham, WA, USA, vol. 1916. pp. 87–96.
[39] B. Wang, Three-dimensional analysis of an ellipsoidal inclusion in a piezoelectric material, Int. J. Solids Structures 29 (1992) 293–308.
[40] Q.M. Zhang, H. Cao, H. Wang, L.E. Cross, Characterization of the performance of 1–3 type piezocomposites for low-frequency applications, J. Appl. Phys. 73 (1993) 1403–1410.
[41] J.D. Eshelby, The determination of the elastic field of an ellipsoidal inclusion, and related problems, Proc. Roy. Soc., A241 (1957) 376–396.